

We are IntechOpen, the world's leading publisher of Open Access books Built by scientists, for scientists

6,900

Open access books available

186,000

International authors and editors

200M

Downloads

Our authors are among the

154

Countries delivered to

TOP 1%

most cited scientists

12.2%

Contributors from top 500 universities



WEB OF SCIENCE™

Selection of our books indexed in the Book Citation Index
in Web of Science™ Core Collection (BKCI)

Interested in publishing with us?
Contact book.department@intechopen.com

Numbers displayed above are based on latest data collected.
For more information visit www.intechopen.com



Properties of Injection Molded High Density Polyethylene Nanocomposites Filled with Exfoliated Graphene Nanoplatelets

Xian Jiang and Lawrence T. Drzal

*Michigan State University, Composite Materials and Structures Center,
Department of Chemical Engineering and Materials Science, East Lansing, Michigan,
USA*

1. Introduction

This book chapter investigated the potential of using exfoliated graphene nanoplatelets, GNP, as the multifunctional reinforcement in high density polyethylene (HDPE) matrix. HDPE/GNP nanocomposites were fabricated by the conventional compounding method of melt-extrusion followed with injection molding. The mechanical properties, crystallization behaviors, thermal stability, thermal conductivity, and electrical conductivity of the resulting HDPE/GNP nanocomposites were evaluated as a function of GNP concentration. Results showed that HDPE/GNP nanocomposites exhibit equivalent flexural modulus and strength to HDPE composites filled with other commercial reinforcements such as carbon fibers (CF), carbon black (CB) and glass fibers (GF). But they have superior impact strength. By investigating the crystallization behavior of HDPE/GNP nanocomposites, it was found that GNP is a good nucleating agent at low loading levels and as a result can significantly increase crystallization temperature and crystallinity of HDPE. At high GNP loadings, however, the close proximity of GNP particles retards the crystallization process. The thermal stability and thermal conductivity of HDPE/GNP nanocomposites were significantly enhanced as a function of GNP concentration due to the excellent thermal properties of GNP. Meanwhile, results indicated that the percolation threshold of these nanocomposites prepared by the conventional melt - extrusion and injection molding is relatively high at around 10-15 vol% GNP loading. The high percolation threshold is mainly due to the severe GNP aggregation and platelets alignment during the processing conditions as verified by the morphology. To enhance their electrical conductivity and lower the percolation threshold, a wax coating method was introduced in this study which is proved to be efficient in improving the dispersion of GNP in HDPE which is responsible for the better electrical and mechanical properties in the resulting nanocomposites.

Polymeric nanocomposites have attracted research interest both in industry and in academia in recent years, they can be found useful in many applications such as electromagnetic interference (EMI) shielding devices, low power rechargeable batteries, electronic devices, light emitting diodes (LEDs), gas sensors, super capacitors and photovoltaic cells (Hussain et al., 2006; Vaia, 2003). Polymeric nanocomposites have represented a radical alternative to

conventional filled polymers or polymer blends. The difference between the conventional fillers and nano-fillers can be explained that nano-reinforcements must have at least one dimension in the nanometer range.

The advantages of using nano-fillers have been summarized in the work by Griffith and Weibull (Griffith, 1920; Weibull, 1951). They claimed that the smaller the reinforcement is, the stronger it becomes. It is believed that the failure of macroscopic specimens is mainly due to the presence of critical size defects. As the material size decreases, the probability of critical size flaws also reduces which allows the material to approach its intrinsic strength. Piggott and Hussain (Hussain et al., 2006; Piggott, 1980) concluded that nano-fillers are more effective reinforcements than their conventional counterparts because a smaller amount of nanoparticles could result in a larger enhancement in the mechanical, electrical, and thermal properties of the polymer matrix.

Recently, carbon nanotubes (CNTs) have been extensively explored as the nano-reinforcement in polymers due to their exceptional mechanical, electrical and thermal properties (Hermant et al., 2009). Many papers have appeared in literature discussing the CNTs-filled polymeric nanocomposites with excellent mechanical, electrical and thermal properties for numerous applications (Balasubramanian & Burghard, 2006; Kim et al., 2005; Singh et al., 2006; Yao et al., 2006). However due to the poor yield and costly fabrication and purifying process, the price of CNTs in the market is still high, which limits the commercial applications of CNTs to date (Kim & Drzal, 2009).

To search for an alternative nano-filler which exhibits the superior properties of CNTs but have a low cost and easy processing, graphite based materials are gaining more and more research attention. Polycrystalline graphite is a material that consists of extended networks of sp^2 -hybridized carbons in a planar layered structure (graphene), leading to excellent thermal and electrical conductivity within this graphitic basal plate. It is found that exfoliation of these graphite layers and dispersion into polymers offers the potential to bring multifunctionality to the host polymers. Furthermore, research has shown that fully exfoliated graphite nanosheets are as effective in conductivity enhancement as CNTs due to their two-dimensional lattice of sp^2 -bond carbon and extremely high aspect ratio (Xie et al., 2008). Based on this principal, a new form of graphite based nano-filler, exfoliated graphene nanoplatelets, has been under investigation in the Drzal group for several years (Fukushima, 2003; Kalaitzidou, 2006). Research has shown that this nano-particle is a potential alternative to other nano-reinforcements such as nano-clays and CNTs since it combines the low cost and layered structure of nano-clays and the superior thermal and electrical properties of CNTs (Jiang & Drzal, 2010,2009,2011; Kalaitzidou et al., 2007). The objective of this book chapter is to: (1) determine the mechanical properties, i.e., flexural strength, flexural modulus, and impact strength of HDPE/GNP nanocomposites made by melt-extrusion and injection molding and their comparison to the HDPE composites reinforced by commercially available fillers such as glass fiber, carbon fiber and carbon black; (2) investigate the crystallization behavior of HDPE with the presence of GNP; (3) explore the thermal stability, thermal conductivity, and electrical conductivity of injection molded HDPE/GNP nanocomposites; (4) observe the morphology of HDPE/GNP nanocomposites to determine the dispersion and orientation of the nano-reinforcement under the melt-extrusion and injection molding conditions; (5) enhance the dispersion of

GNP in HDPE by a wax coating method which is suitable for melt-extrusion and injection molding.

2. Experimental

2.1 Materials

In this book chapter, HDPE pellets with the trade name Marlex® HXM 50100 (Density 0.948 g/cm³, MW~ 230,000) were obtained from Chevron Phillips Chemical Company. Paraffin wax (max C30, Density 0.92 g/cm³, MW~ 500) with the melting point of 55°C was purchased from Sigma-Aldrich. GNP nanoplatelets were obtained from XG Science, Inc (www.xgsciences.com). There are two kinds of GNP particles used in this study. GNP-1 has the thickness of around 5-10nm and a platelet diameter of 1 μm; while GNP-15 has the same thickness but the diameter is around 15 μm.

Several commercial reinforcements and fillers were also combined with HDPE to make composites for comparison to the HDPE/GNP nanocomposites. They are: (1) CF-PAN based carbon fiber (PANEX 33 MC Milled Carbon Fibers, Zoltek Co), (2) CB-nanosize 'High Structure' carbon black (KETJENBLACK EC-600 JD, Akzo Novel Polymer Chemicals LLC), and (3) GF-chopped glass fiber (StarStran® LCF, Johns Manville Co.) . The physical properties of these materials are detailed in Table 1.

Filler	Length (μm)	Diameter (μm)	Aspect Ratio	Surface Area (m ² /g)	Density (g/cm ³)
GNP-1	<0.01	1	<100	100	2.1
GNP-15	<0.01	15	~1500	40	2.1
PAN CF	175	7.2	~24	16	1.8
GF	51 (mm)	13	~4000	NA	2.6
CB	0.4 - 0.5	0.4 - 0.5	1	1400	1.8

Table 1. Geometrical and surface characteristics of various fillers.

2.2 Processing methods

Melt - extrusion of HDPE/GNP nanocomposites was carried out in a DSM Micro 15cc Compounder, (Vertical, co-rotating, twin-screws micro-extruder) operating at 220°C for 5 minutes at a screw speed of 100rpm. The composite melt was then transferred to a Daga Micro injector with the T_{barrel}=220°C and T_{mold}=90°C. The injection pressure applied for the injection molding of flexural coupons was at 0.6MPa. Round disks (thickness ~1.5mm, diameter ~25mm) were also injection molded for thermal conductivity test under the same injection conditions. The melt - extrusion and injection molding systems are shown in the Fig. 1.

To enhance the dispersion of GNP in the HDPE matrix, a wax coating technique was applied in this study, which uniformly coated the surface of GNP with wax. For this method, wax was first dissolved in xylene at around 60°C and GNP was added afterwards. Sonication was then applied for 30 minutes at 100W to initially break down the GNP aggregates and to ensure a uniform wax coating. The resultant mixture was poured into an aluminum pan and left in a hood at room temperature to evaporate the solvent. After xylene was completely evaporated, the wax coated GNP was further dried in a vacuum oven

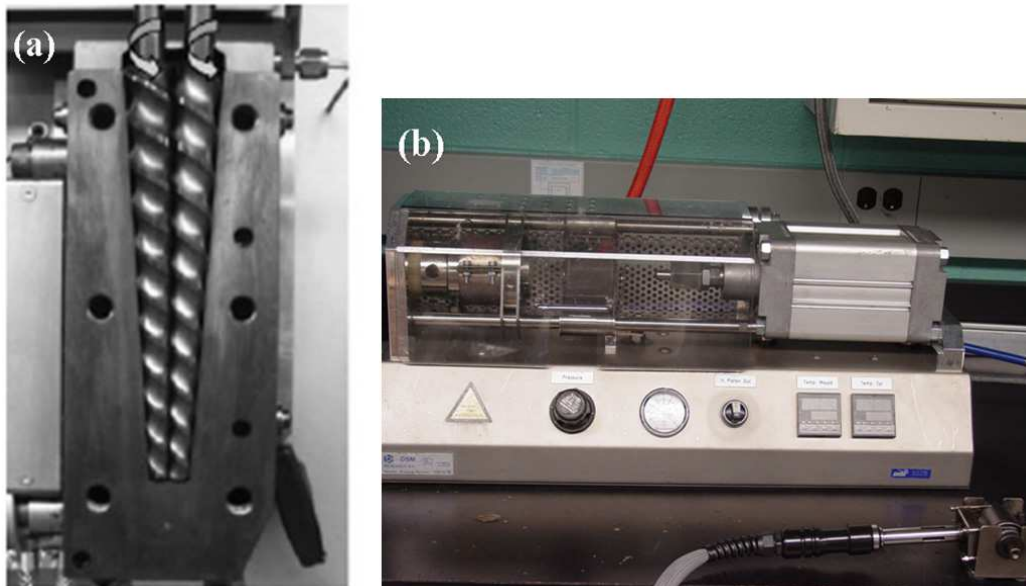


Fig. 1. (a) A DSM Micro 15cc Compounder, (Vertical, co-rotating, twin-screws microextruder); (b) A Daka Micro injector.

overnight at 30°C. In this study, four different wax coated GNP-15 samples were prepared having wax to GNP-15 ratios of 5:95, 10:90, 20:80, and 30:70wt%. This procedure of producing wax coated GNP is schematically shown in the Fig. 2.

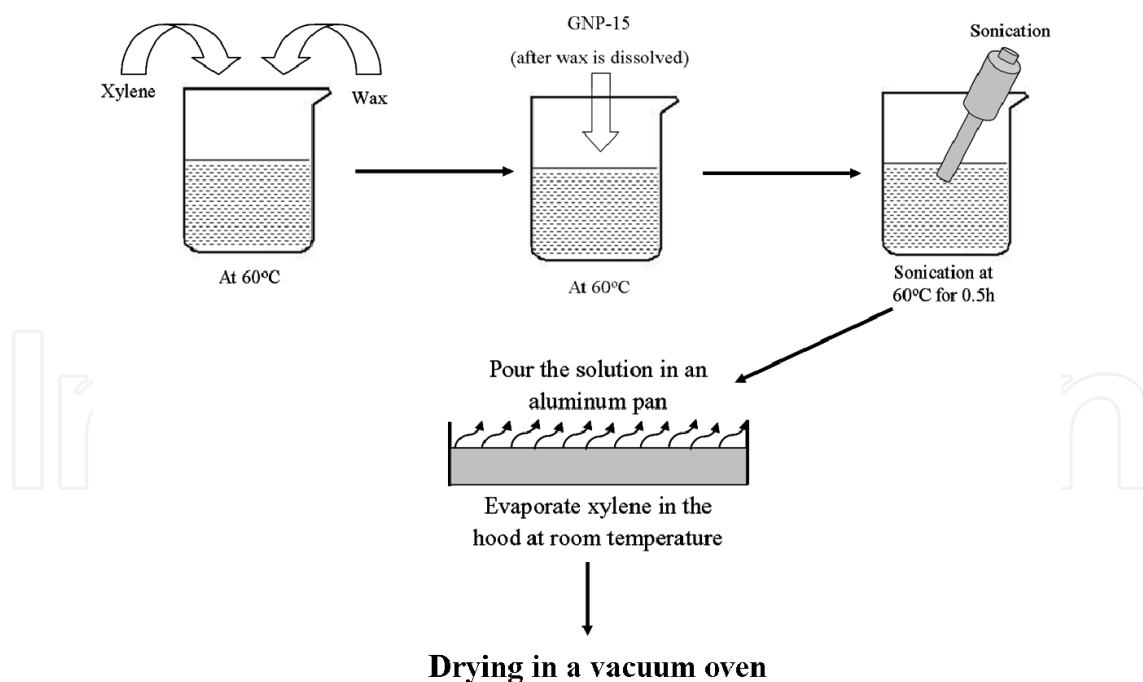


Fig. 2. The procedure of producing wax coated GNP-15.

Then wax coated GNP-15 was re-dispersed in HDPE by melt - extrusion in the DSM Micro 15cc Compounder with the same processing parameters described above. The actual loading of GNP-15 in the final nanocomposites was kept at 5vol%. After extrusion, the resulting

HDPE/wax coated GNP-15 (HDPE/WaxGNP-15) composite melts were injection molded into flexural coupons for mechanical and electrical properties test. The sample nomenclature for HDPE/WaxGNP-15 nanocomposites with different wax to GNP-15 ratios is: 5vol% HDPE/WaxGNP-15 (20:80wt%) means the actual GNP-15 loading in this nanocomposite is 5vol% and the weight ratio between wax and GNP-15 is 20:80.

To exclude any artifact due to the sonication, GNP-15 was added into xylene with the same sonication time of 30 minutes but without the addition of wax. After complete evaporation of xylene, GNP-15 was melt mixed with HDPE by the same melt - extrusion and injection molding process to obtain the HDPE/GNP-15 (sonic.) nanocomposites with GNP-15 loading at 5vol% as a reference.

2.3 Characterization techniques

Flexural tests were performed with a UTS SFM-20 machine (United Calibration Corp.) at room temperature by following the ASTM D790 standard test method (3-point bending mode). The test was performed at a flexural rate of 0.05 in/min. Impact strength tests (Izod impact type) were performed following the ASTM D256 standard test method.

The crystallinity and crystallization temperature were measured by using Dynamic Scanning Calorimetry (DSC Q2000, TA instrument). The samples used were 5–10 mg and non-isothermal crystallization was studied using the following experimental conditions: the sample was heated to 160°C at a rate of 20°C/min. The prior thermal history of the sample was erased by maintaining isothermal conditions at 160°C for 5 minutes. Then the sample was cooled down to 40°C at a rate of 20°C/min, held isothermally for 5 minutes and reheated at 20°C/min to 160°C and cooled back to 40°C again. The data of melting enthalpy (ΔH_m) and crystallization peak temperature (T_c) were collected during the second cycle. The degree of crystallization was calculated by the following equation, where $\chi\%$ is the percent crystallinity of the matrix, wt% is the weight percentage of GNP, and ΔH_m^0 is the theoretical melting enthalpy of the polymer matrix if it is 100% crystalline.

$$\chi\% = \frac{1}{1 - \text{wt}\%} \frac{\Delta H_m}{\Delta H_m^0} \quad (1)$$

The thermal stability of HDPE/GNP nanocomposites was determined from the thermogravimetric analysis (TGA), which was carried out on a TA instrument (TGA 2950) at a heating rate of 20°C/min under nitrogen from 30°C to 800°C. Thermal diffusivity (a , m²/s) of GNP nanocomposites (round disks) was measured by a LFA Nanoflash 447 Light flash system. To calculate the thermal conductivity, the bulk density of the samples (ρ , kg/m³) was obtained by dividing the mass over the volume, and the specific heat capacity (C_p ; J/(kg · K)) was measured through the Dynamic Scanning Calorimetry (DSC Q2000, TA instrument). The thermal conductivity (κ , W/(m · K)) of GNP samples was then calculated by the following equation:

$$\kappa = a \times \rho \times C_p \quad (2)$$

The electrical resistivity of HDPE/GNP nanocomposites was measured both along the material flow direction (in-plane resistivity) and through the sample thickness direction (through-plane resistivity, normal to the flow direction), using the impedance spectroscopy

by applying a two-probe method at room temperature. Samples with dimensions of 10.0 x 3.2 x 12.2mm (Length x Thickness x Width) were cut from the middle portion of flexural coupons. The two surfaces connected to the electrodes were first treated with O₂ plasma (14mins, 375W) in order to remove the top surface layers which are rich in polymer and then conductive silver paste was applied to the surface to ensure a good contact with the electrodes. The resistance of samples was measured and converted to resistivity by taking the sample dimensions into account.

The preparation of SEM samples in this study included epoxy mounting, grinding, polishing and etching steps. First, specimens were mounted with epoxy in cylindrical sample holders to maintain a flat surface over the entire grinding and polishing area. After epoxy was fully cured, samples were carefully grounded and polished. O₂ plasma etching (25mins, 375W) was then applied at the last step to remove the polymer in top surface allowing the GNP platelets to stand out under the SEM observation. A JEOL (model JSM-6400) SEM was then used to characterize the dispersion of GNP in HDPE. Samples were also gold coated to avoid charging.

3. Results and discussion

3.1 Flexural and impact properties of HDPE/GNP nanocomposites made by melt-extrusion and injection molding and the comparison of GNP to other reinforcements

The flexural strength and flexural modulus of HDPE/GNP nanocomposites and their comparison to HDPE composites filled with other reinforcements are presented in the Fig. 3 and Fig. 4 (Jiang & Drzal, 2010) respectively. All filler concentrations are from 0vol% to 15vol% except CB. HDPE/CB composites with CB concentration higher than 5vol% are not included because at the given processing conditions, the viscosity of these composites increases to the

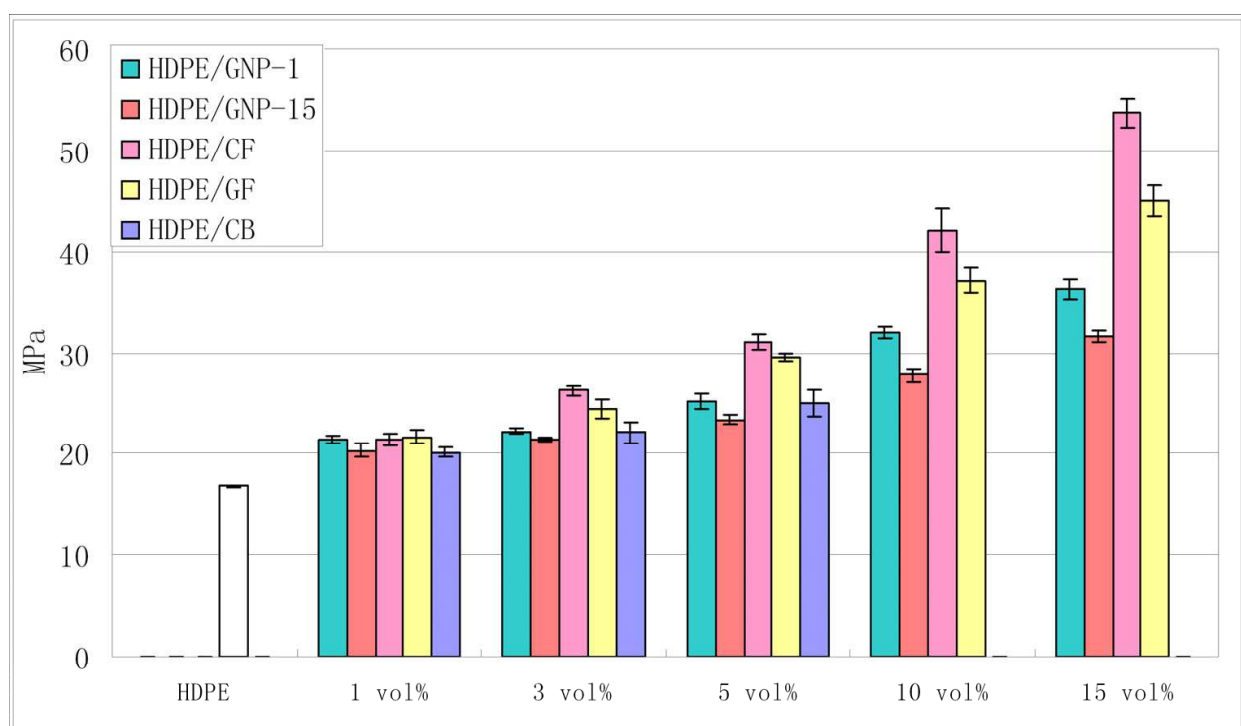


Fig. 3. Flexural strength of various HDPE composites.

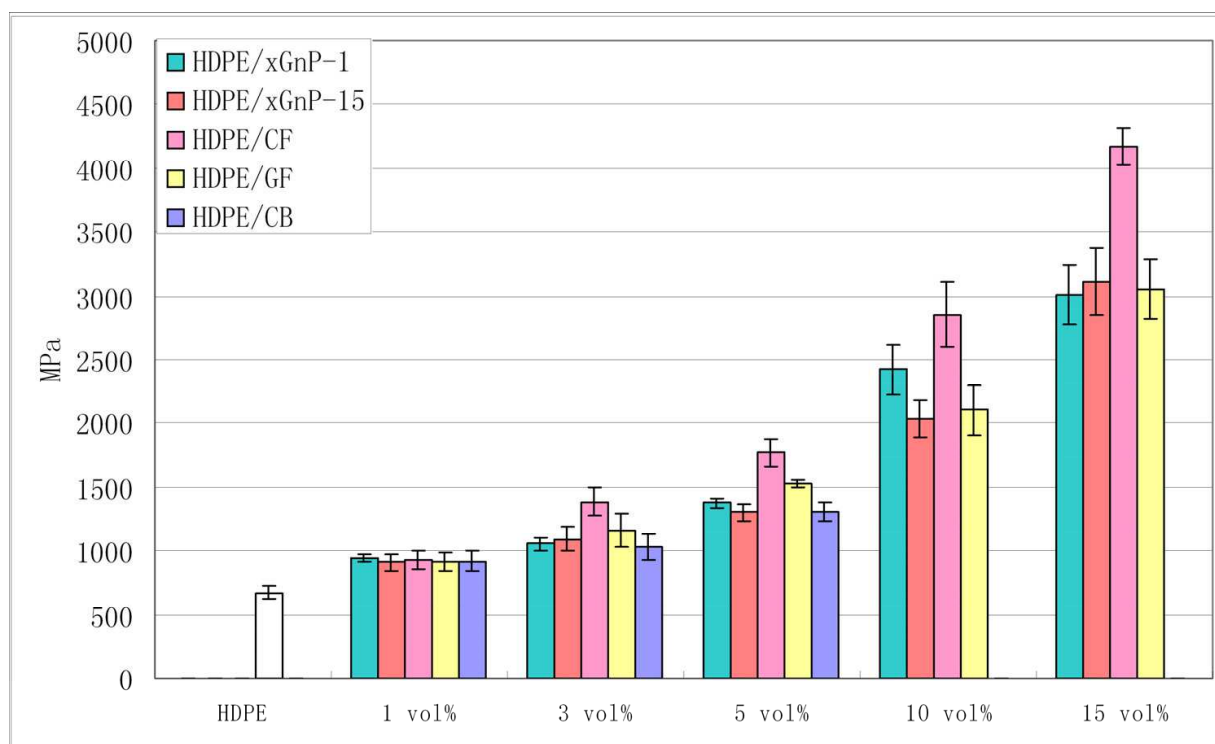


Fig. 4. Flexural modulus of various HDPE composites.

level where the DSM extruder could not generate sufficient pressure to extrude the mix properly. For the flexural strength shown in the Fig. 3, HDPE/CF composites exhibit the highest improvement at all filler loading levels followed by HDPE/GF composites. At the highest loading of 15vol%, HDPE/CF and HDPE/GF result in ~220% and ~170% improvement in flexural strength compared to the neat HDPE respectively. The great enhancement in the flexural strength for HDPE/CF and HDPE/GF composites is largely due to the high aspect ratio and excellent flexural properties of these carbon and glass fibers (Mai et al., 1994). HDPE/GNP nanocomposites also exhibit a significant increase in flexural strength with the increasing of GNP content. At 15vol% GNP loading, HDPE/GNP-1 and HDPE/GNP-15 nanocomposites result in ~116% and ~90% improvement in flexural strength respectively. Meanwhile, it is detected that GNP-1 nanocomposites are superior to GNP-15 counterparts in flexural strength at every GNP loading. At low CB concentrations up to 5vol%, HDPE/CB composites have the flexural strength value close to those of HDPE/GNP-1 samples. And as seen for the flexural modulus of these composites presented in the Fig. 4, HDPE/CF composites display the greatest enhancement in flexural modulus. HDPE/GNP nanocomposites are competitive to their HDPE/GF and HDPE/CB (up to 5vol%) counterparts.

The Izod impact strength of various HDPE composites up to a filler loading of 15vol% is displayed in the Fig. 5. (Jiang & Drzal, 2010). A reduction in impact strength is observed in all HDPE composites compared to the neat HDPE which is the case normally accompanies incorporation of a rigid filler into a relatively tough polymer (Wakabayashi et al., 2008). However, it is noted that HDPE/GNP nanocomposites exhibit the smallest reduction, which implies the advantage of using GNP as the reinforcement. At the filler loadings from 1vol% to 15vol%, overall HDPE/GNP-1 nanocomposites have the highest impact strength

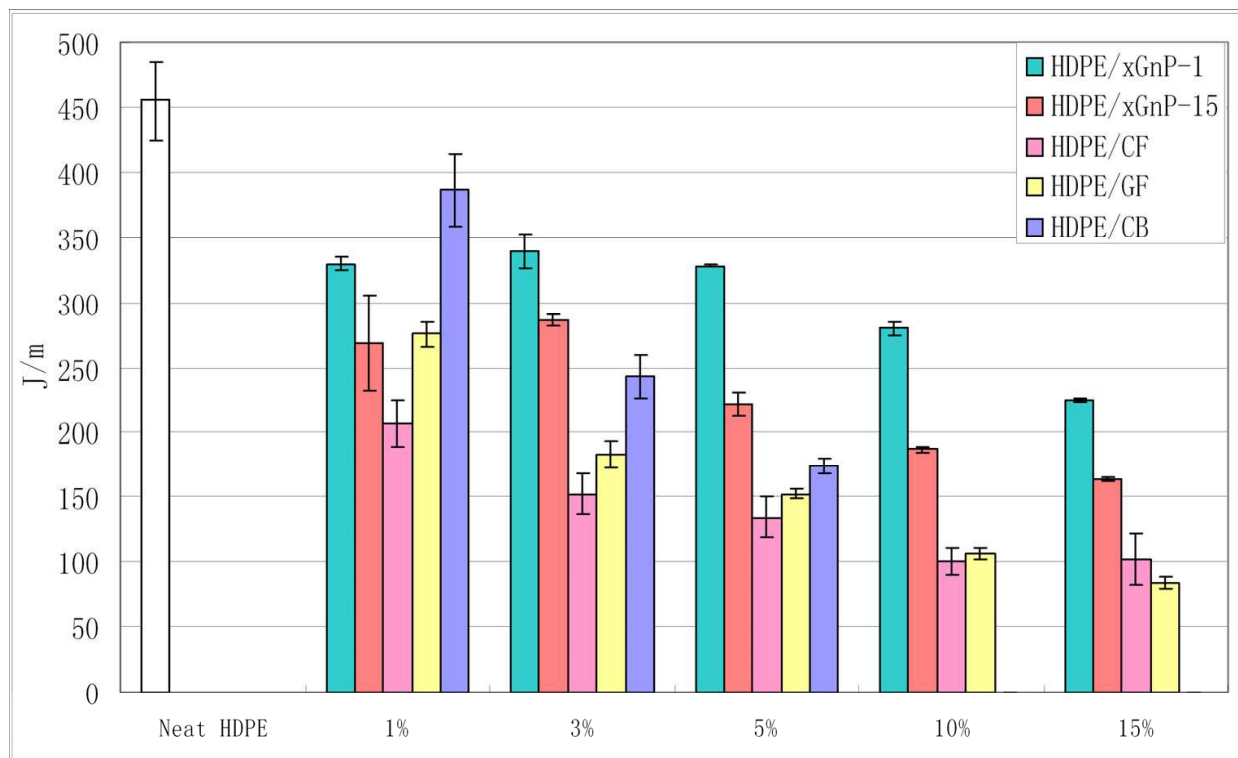


Fig. 5. Impact strength of various HDPE/GNP nanocomposites.

followed by HDPE/GNP-15 nanocomposites and then HDPE/CB composites (up to 5vol%). HDPE/CF and HDPE/GF show inferior performance compared to the other composites. The difference in impact strength may result from the difference in reinforcement size and aspect ratio, difference in dispersion of reinforcements in the polymer matrix and the difference in the adhesion between the reinforcements and the polymer matrix (Kim & Mai, 1991). Those differences eventually result in the different energy absorbing mechanisms at the impact fracture surface.

3.2 Crystallization behavior of HDPE/GNP nanocomposites made by melt-extrusion and injection molding

The crystallization temperature of HDPE/GNP nanocomposites with the GNP loading up to 15vol% is shown in the Fig. 6. It is concluded that incorporation of GNP has a significant effect on the crystallization temperature of HDPE, that is, the crystallization temperature increases as the GNP content increases. A relatively large temperature increase can be detected (around 3°C) even at a low GNP loading of 1vol%. The increased crystallization temperature suggests that the presence of GNP particles acts as nucleating agents which facilitate the crystallization process of HDPE (Peneva & Minkova, 2006).

The total percent of crystallinity of HDPE/GNP-1 and HDPE/GNP-15 nanocomposites obtained from equation [1] after the non-isothermal crystallization process is presented in the Fig. 7. It is interesting to note that the crystallinity value of GNP-1 and GNP-15 nanocomposites first increases with the GNP content and then it drops to an almost constant value. The highest crystallinity of HDPE/GNP-1 and HDPE/GNP-15 nanocomposites both occurs at 3vol% GNP loading. This interesting phenomenon is believed to be the result of a

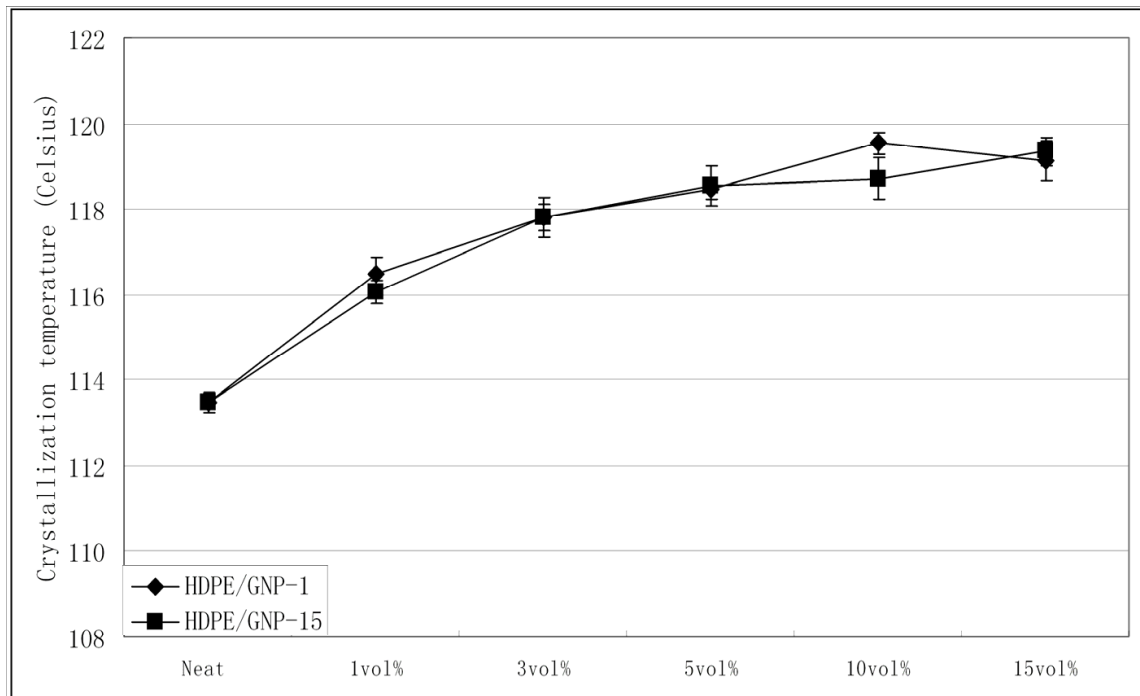


Fig. 6. Crystallization temperature of HDPE/GNP nanocomposites.

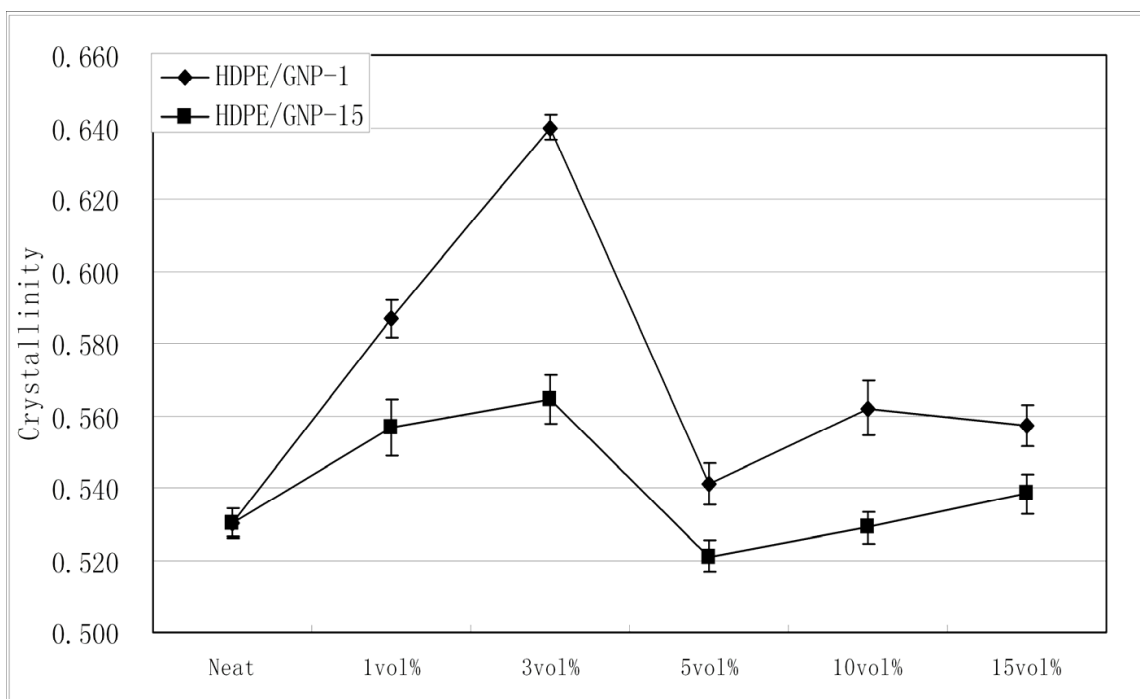


Fig. 7. Total percent of crystallinity of HDPE/GNP nanocomposites.

compromise between the nucleating and retarding effects of GNP on the host polymer during the non-isothermal crystallization (Di Maio et al., 2004). When the GNP content is relatively low, GNP particles exhibit a strong nucleating effect and act as heterogeneous nucleating sites at the GNP-HDPE interfaces, thus increasing the total percent of

crystallinity of HDPE. And if the GNP concentration reaches a high level, the presence of the abundant GNP particles significantly hinders the diffusion of polymer chains to the growing crystallites. The crystallinity is therefore reduced. From the Fig. 7, it is also seen that HDPE/GNP-1 nanocomposites always show higher crystallinity than HDPE/GNP-15 counterparts at the same GNP loading, which indicates the nucleating efficiency between GNP-1 and GNP-15 is different. The superior nucleating efficiency of GNP-1 is due to the fact that the absolute number of GNP-1 particles is much larger than GNP-15 at the same filler concentration which provides more heterogeneous nucleating sites to initiate the polymer crystallization (Jiang & Drzal, 2011).

3.3 Thermal stability and thermal conductivity of HDPE/GNP nanocomposites made by melt-extrusion and injection molding

Fig. 8 and Fig. 9 present the TGA curves for HDPE/GNP-1 and HDPE/GNP-15 nanocomposites with different GNP loadings in nitrogen respectively. From the thermogravimetric curves, it is seen the pure HDPE is relatively thermal stable until around 300°C and after the onset degradation temperature of around 420°C, the degradation rate accelerates. However, for HDPE/GNP-1 nanocomposites, the onset degradation temperature increases from 420°C for neat HDPE to around 500°C for the sample at 15vol% GNP loading. Significant increase in onset degradation temperature suggests that the thermal stability of HDPE/GNP-1 nanocomposites is substantially enhanced, which is due to the high thermal stability of GNP-1 and the shielding effect of GNP-1 on the diffusion of combustion gases into and out of the polymer matrix during its thermal decomposition (Yang et al., 2007). A largely enhanced thermal stability can also be observed in HDPE/GNP-15 nanocomposites, where the onset thermal decomposition temperature is increased by around 70°C from neat HDPE to the HDPE/GNP-15 sample at 15vol% filler loading.

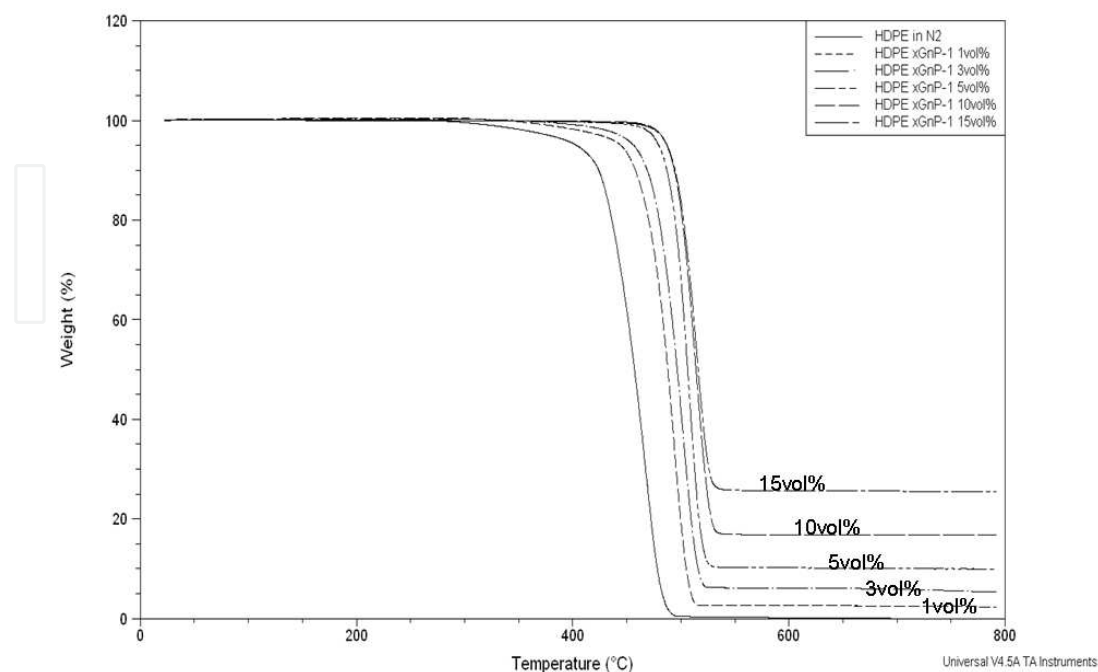


Fig. 8. TGA curves of HDPE and HDPE/GNP-1 nanocomposites.

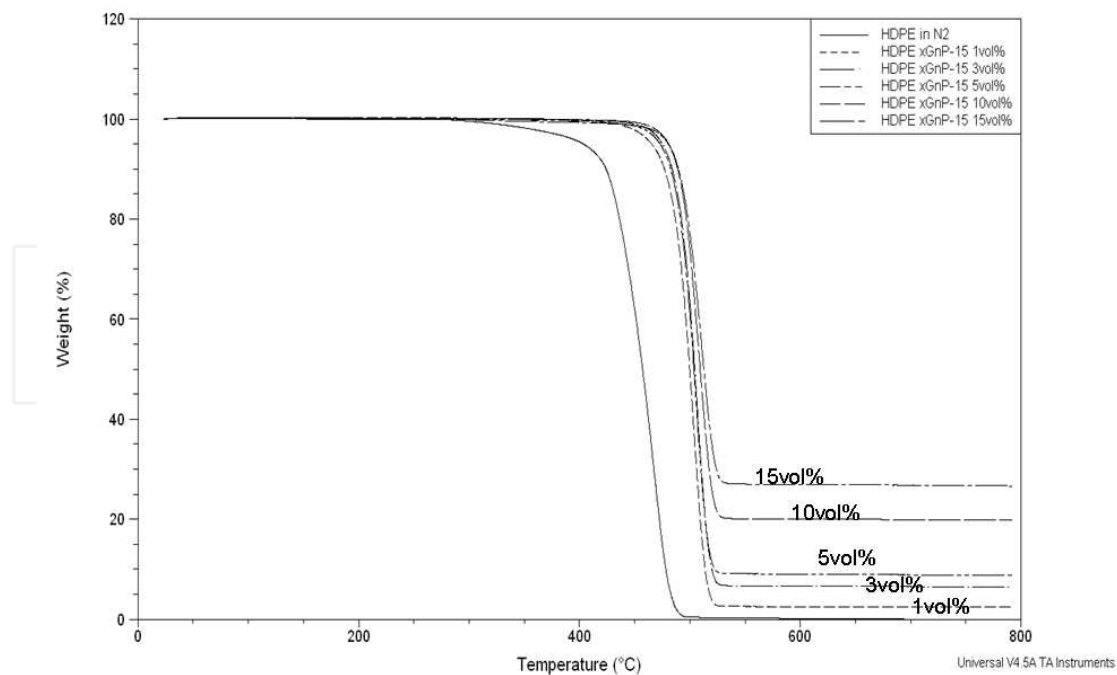


Fig. 9. TGA curves of HDPE and HDPE/GNP-15 nanocomposites.

The in-plane as well as the through-plane thermal conductivity of HDPE/GNP nanocomposites calculated by the equation [2] is characterized in the Fig. 10. As the GNP loading increases, it is detected that both the in-plane and through-plane thermal conductivity of HDPE/GNP nanocomposites undergo a substantial increase. At relatively

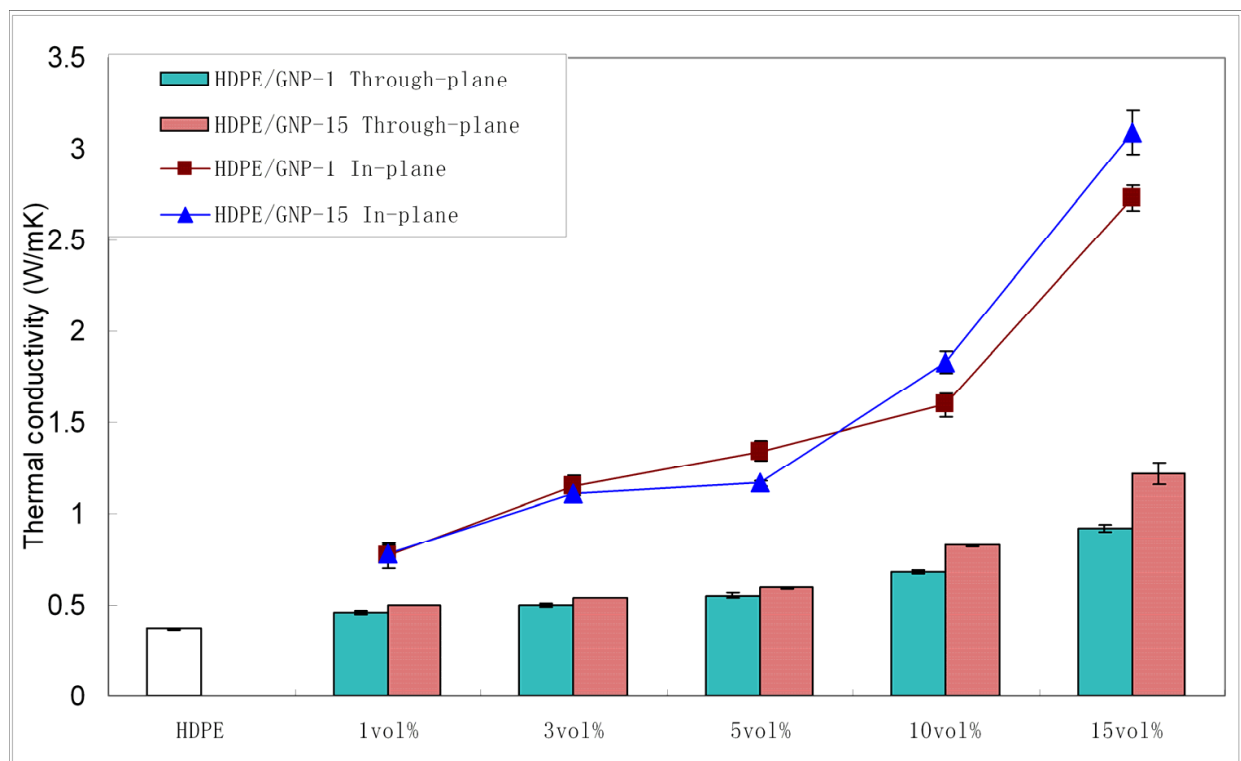


Fig. 10. Thermal conductivity of HDPE/GNP nanocomposites.

low GNP contents (1-5 vol%), HDPE/GNP-15 nanocomposites exhibit a thermal conductivity that is almost the same as that of HDPE/GNP-1 counterparts. When the GNP loading is higher than 5vol%, however, HDPE/GNP-15 nanocomposites show both superior in-plane and through-plane thermal conductivity. The higher thermal conductivity in GNP-15 samples is due to the larger aspect ratio of GNP-15 particles, which makes them more easily to connect with each other in forming conductive pathways thus reducing the thermal contact resistance and increasing the thermal conductivity of the resulting HDPE/GNP-15 nanocomposites.

If we compare the in-plane conductivity with the through-plane conductivity, it is found HDPE/GNP nanocomposites exhibit a much higher in-plane thermal conductivity at every GNP loading. For injection molded HDPE/GNP samples, higher in-plane conductivity is resulted from the preferential GNP alignment during the injection molding process, which will be fully addressed later in the morphology section and the anisotropic thermal property of GNP itself (The in-plane thermal conductivity of GNP platelet is 3000W/mK, and the through-plane conductivity is only 10W/mK due to its anisotropic structure (Kalaitzidou, 2006)).

3.4 Electrical conductivity of HDPE/GNP nanocomposites made by melt-extrusion and injection molding

The in-plane and through-plane electrical resistivity of HDPE/GNP nanocomposites made by melt-extrusion and injection molding are shown in the Fig. 11. For both in-plane and through-plane resistivity, it is seen that between 10vol% and 15vol% GNP content, there is a large decrease in the resistivity. This concentration range (10-15vol%) is thus noted as the percolation threshold for HDPE/GNP nanocomposites. The percolation threshold is defined as the concentration where a connected assembly of conductive particles

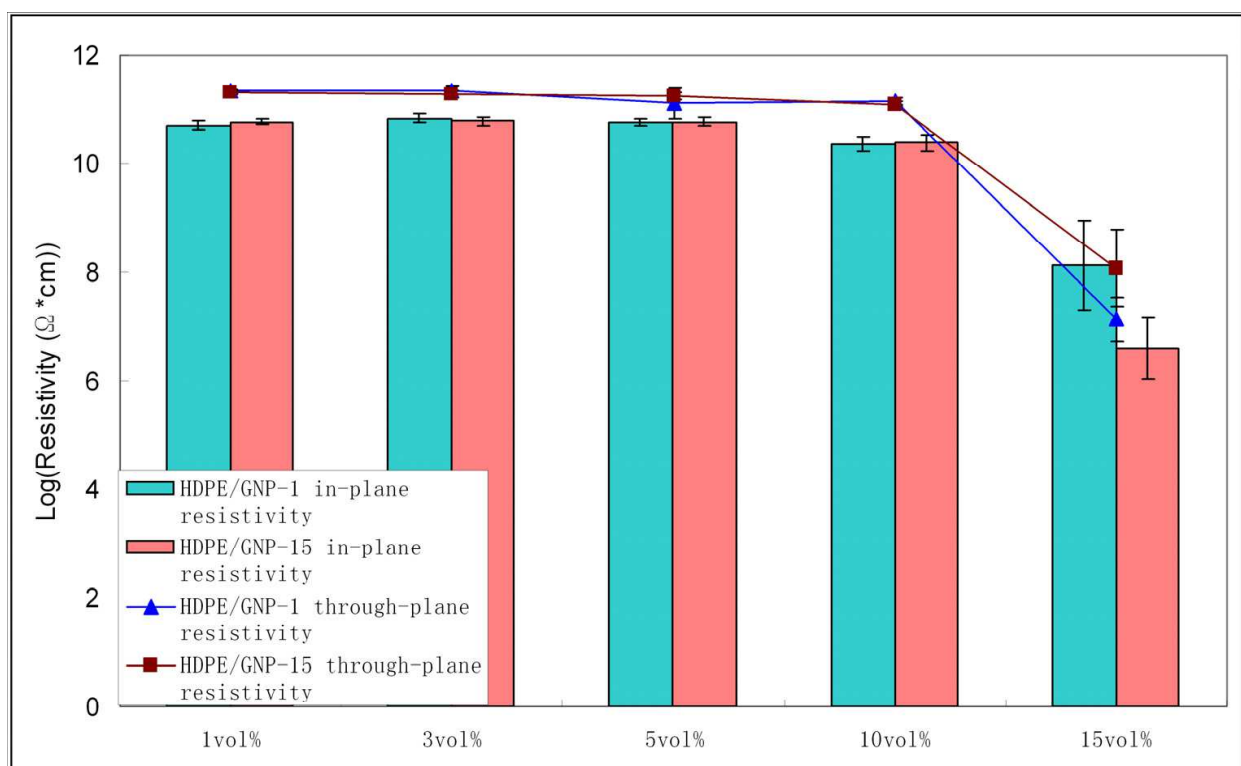


Fig. 11. In-plane and through-plane electrical resistivity of HDPE/GNP nanocomposites.

is formed within a polymer matrix. This assembly penetrates throughout the sample in forming conductive paths for electron transportation. At this concentration of the conductive filler, the electrical conductivity of the nanocomposites significantly increases and the nanocomposites become electrical conductive (I. Krupa et al., 2004).

Interestingly, at the GNP concentration of 15vol% (higher than the percolation threshold), HDPE/GNP-15 nanocomposites exhibit a lower in-plane electrical resistivity than HDPE/GNP-1 samples, which means HDPE/GNP-15 nanocomposites are more electrical conductive. However, at this GNP loading, HDPE/GNP-1 samples show a slightly higher through-plane electrical conductivity. By comparing the in-plane resistivity with the through-plane resistivity, it is concluded that HDPE/GNP-1 and HDPE/GNP-15 nanocomposites both exhibit a higher in-plane electrical conductivity, which is due to the platelet structure of GNP particles and the anisotropic property of injection molded composites as described above for the thermal conductivity. During injection molding, GNP platelets are aligned parallel to each other along the material flow direction, and at certain loading levels will they start intersecting with each other to form a conductive path. Because of the platelet morphology, aligned GNP particles are more difficult to get contact with each other through the thickness direction, thus leading to higher through-plane resistivity or lower electrical conductivity.

From the literature, it is noted that GNP nanocomposites fabricated by other processing methods such as solution compounding, pre-mixing, solid state ball milling, and solid state shear pulverization tend to have lower percolation threshold or higher electrical conductivity than the samples made by melt-extrusion and injection molding in this study (Jiang & Drzal, 2011; Kalaitzidou et al., 2007). The high percolation threshold is a result of the GNP aggregation during melt - extrusion and preferential platelets alignment in the injection molding process due to the large aspect ratio and planar shape of GNP, which will be fully explored in the next section.

3.5 Morphology of HDPE/GNP nanocomposites made by melt-extrusion and injection molding

The morphology of HDPE/GNP-1 and HDPE/GNP-15 nanocomposites fabricated by melt-extrusion and injection molding is presented in the Fig. 12. The samples at 5vol% GNP loading were taken as an example. Images (a) and (c) show the injection molded morphology near the mold wall or at the edge, where the shear forces under the injection molding conditions is high. And images (b) and (d) represent the injection molded morphology in the center of the composites, where the shear force is small. From the images of (a) and (c), it is concluded that all the GNP-1 and GNP-15 particles align parallel along the material flow direction and they are totally separated by the polymer matrix. Meanwhile, large GNP aggregates can be observed in these two images, especially in the GNP-15 sample, which is the indication of insufficiency of DSM extrusion for good GNP separation and dispersion. The presence of these large GNP aggregates drastically reduces the number of GNP platelets available as 'effective' reinforcing particles and significantly decreases the probability of interconnections between GNP platelets in forming electrically conductive pathways. Therefore, the high percolation threshold or low electrical conductivity in melt-extrusion and injection molded HDPE/GNP nanocomposites could be attributed to the severe GNP aggregation and preferential GNP alignment during the melt-extrusion and

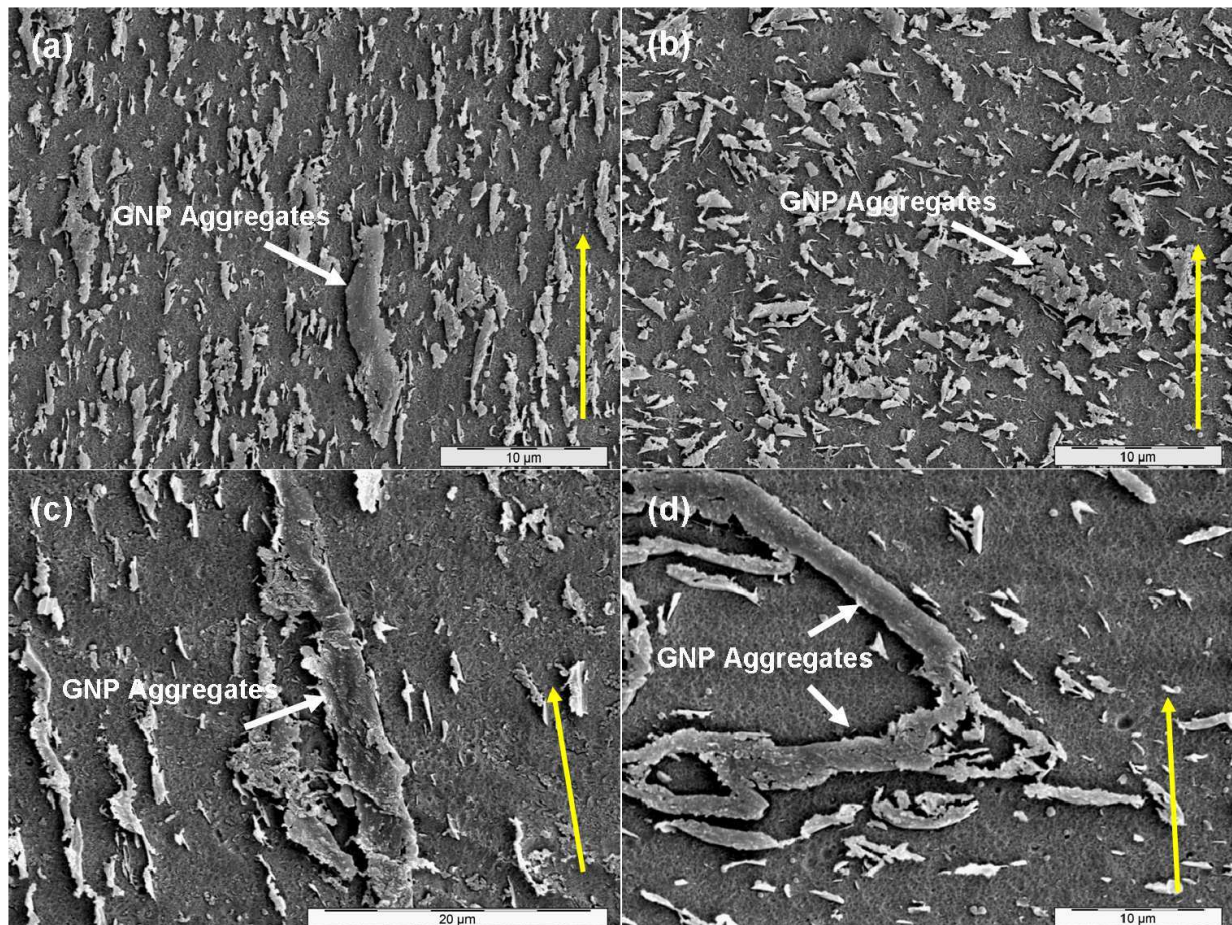


Fig. 12. Morphology of HDPE/GNP nanocomposites made by melt-extrusion and injection molding. The GNP loading is 5vol%. (a) GNP-1 sample at the edge; (b) GNP-1 sample in the center; (c) GNP-15 sample at the edge; (d) GNP-15 sample in the center. The yellow arrow on the right bottom indicates the material flow direction during injection molding.

injection molding process. The aligned structure of GNP platelets in the resulting nanocomposites also leads to much higher in-plane thermal and electrical conductivity as described above. Meanwhile, it is detected that the number density of GNP-1 particles are much larger than that of GNP-15 at the same GNP loading due to their smaller size, which is considered as a major reason of higher flexural strength, impact strength, and crystallinity in the resulting GNP-1 nanocomposites.

Compared with the morphology at the edge, it is found that GNP platelets in the center of the composites (images (b) and (d)) do not exhibit preferential alignment along the material flow direction. They are randomly oriented because of the minimum shear forces encountered during injection molding. However, large GNP aggregates can also be observed which further confirm the insufficient shear force attainable in the DSM extrusion to break down the GNP aggregates and to achieve a uniform GNP dispersion.

In summary, GNP nanoplatelets tend to align along the material flow direction at the edge of injection molded nanocomposites while they are randomly oriented at the center. The presence of large GNP aggregates constrains the fully translation of superb mechanical and electrical properties of GNP particles into good mechanical and electrical properties of the resulting nanocomposites.

3.6 Wax coating method to improve the dispersion of GNP in HDPE

To improve the dispersion of GNP particles in melt-extrusion and injection molded HDPE/GNP nanocomposites, the wax coating method was applied which is based on the steric repulsion force between the wax coated GNP nanoplatelets in preventing the aggregation of GNP during the processing conditions. Take the GNP-15 nanocomposites for example, the in-plane and through-plane electrical resistivity of HDPE/WaxGNP-15 nanocomposites with different wax to GNP weight ratios are displayed in the Fig. 13. (Jiang & Drzal, 2011). The GNP loading in all these nanocomposites is kept at 5vol%. Interestingly, with the presence of wax coated on the surface of GNP, the previous non-conductive 5vol% HDPE/GNP-15 nanocomposite (control sample) becomes electrical conductive along the material flow direction. And the in-plane resistivity is continuously decreased as the wax content increases. A more than 5 orders of magnitude decrease in resistivity is seen from the control sample to the 5vol% HDPE/WaxGNP-15 (30:70wt%) nanocomposite, suggesting that the electrical conductivity of HDPE/WaxGNP-15 nanocomposites is significantly enhanced. Therefore, the percolation threshold of injection molded HDPE/GNP-15 nanocomposites is reduced from the previous 10-15vol% GNP loading to less than 5vol%. However, the through-plane electrical resistivity of these nanocomposites remains high and it is unaffected by the addition of the wax.

Meanwhile, if we compare the resistivity value of the sonicated sample (5vol% HDPE/GNP-15 (sonic.)) with the control sample, no significant difference in resistivity is observed. This implies that the application of sonication alone without the use of wax is insufficient to improve the electrical conductivity of the resulting nanocomposites.

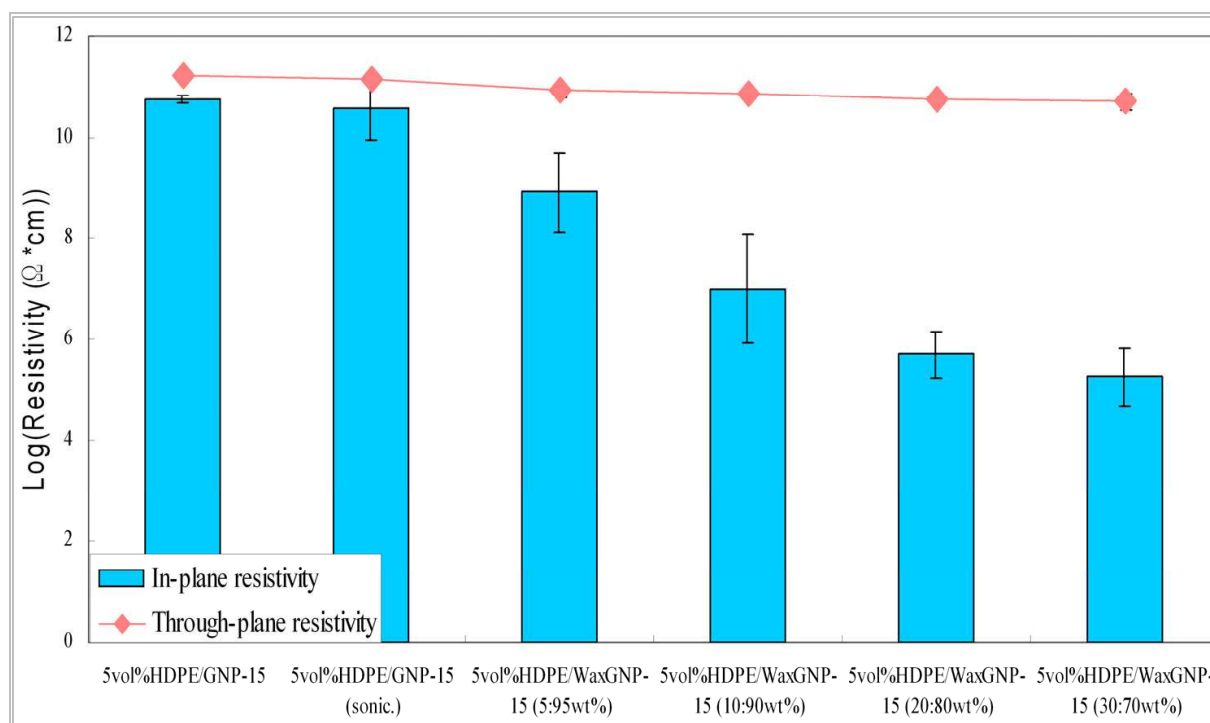


Fig. 13. In-plane and through-plane electrical resistivity of various HDPE/WaxGNP-15 nanocomposites at 5vol% GNP loading made by melt-extrusion and injection molding.

Fig. 14 (Jiang & Drzal, 2011) gives the flexural properties of various HDPE/WaxGNP-15 nanocomposites at 5vol% GNP loading. It is found that as the amount of wax coating on the

GNP surface increases, both the flexural strength and flexural modulus of the resulting nanocomposites firstly increase and then the trend reverses. The largest enhancement in the flexural properties is detected at the 5vol% HDPE/WaxGNP-15 (20:80wt%) sample, of which the flexural strength is increased by 12% and the flexural modulus is improved by 20%. Higher flexural strength and modulus is a strong indication of an improved GNP dispersion in HDPE (Kashiwagi et al., 2007). And the reduction in mechanical properties in the 5vol%HDPE/WaxGNP-15 (30:70wt%) nanocomposite could be explained as the addition of too much low molecular weight polyethylene (wax) into the nanocomposite, which compromises the positive effect of enhanced GNP dispersion on the mechanical strength (Jiang & Drzal, 2011). Again, we do not see any enhancement in flexural properties for the sonicated sample.

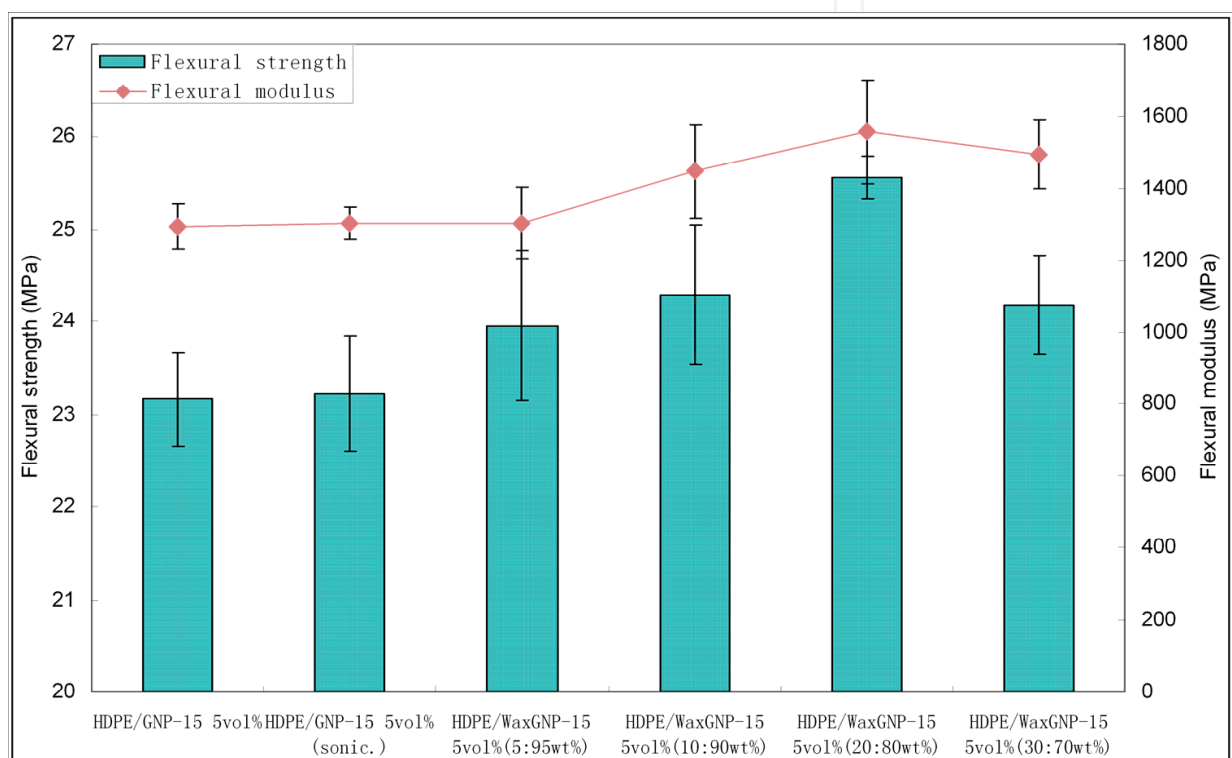


Fig. 14. Flexural strength and flexural modulus of various HDPE/WaxGNP-15 nanocomposites at 5vol% GNP loading made by melt-extrusion and injection molding.

The morphology of these nanocomposites at the edge is presented in the Fig. 15 (Jiang & Drzal, 2011), which helps to explain the substantial improvement in electrical and mechanical properties for HDPE/GNP-15 nanocomposites made by the wax coating method. As discussed in the previous section, GNP-15 platelets in the control sample are aligned along the material flow direction and large GNP-15 aggregates are present (Fig. 12(c)). From the Fig. 15(a), which is the morphology of the sonicated sample, a similar morphology can be seen, that is, there exhibit preferential GNP-15 alignment and large GNP-15 aggregates. This similarity in morphology between the sonicated sample and the control sample suggests that sonication alone without wax is not sufficient to improve the dispersion of GNP-15 in HDPE. Although the technique of sonication is proved as an efficient method to break down the agglomerates or aggregates of nano-particles (Bang & Suslick, 2010) in solution, once incorporated in polymers, these nano-particles which were initially separated would like to re-aggregate again during the melt processing conditions.

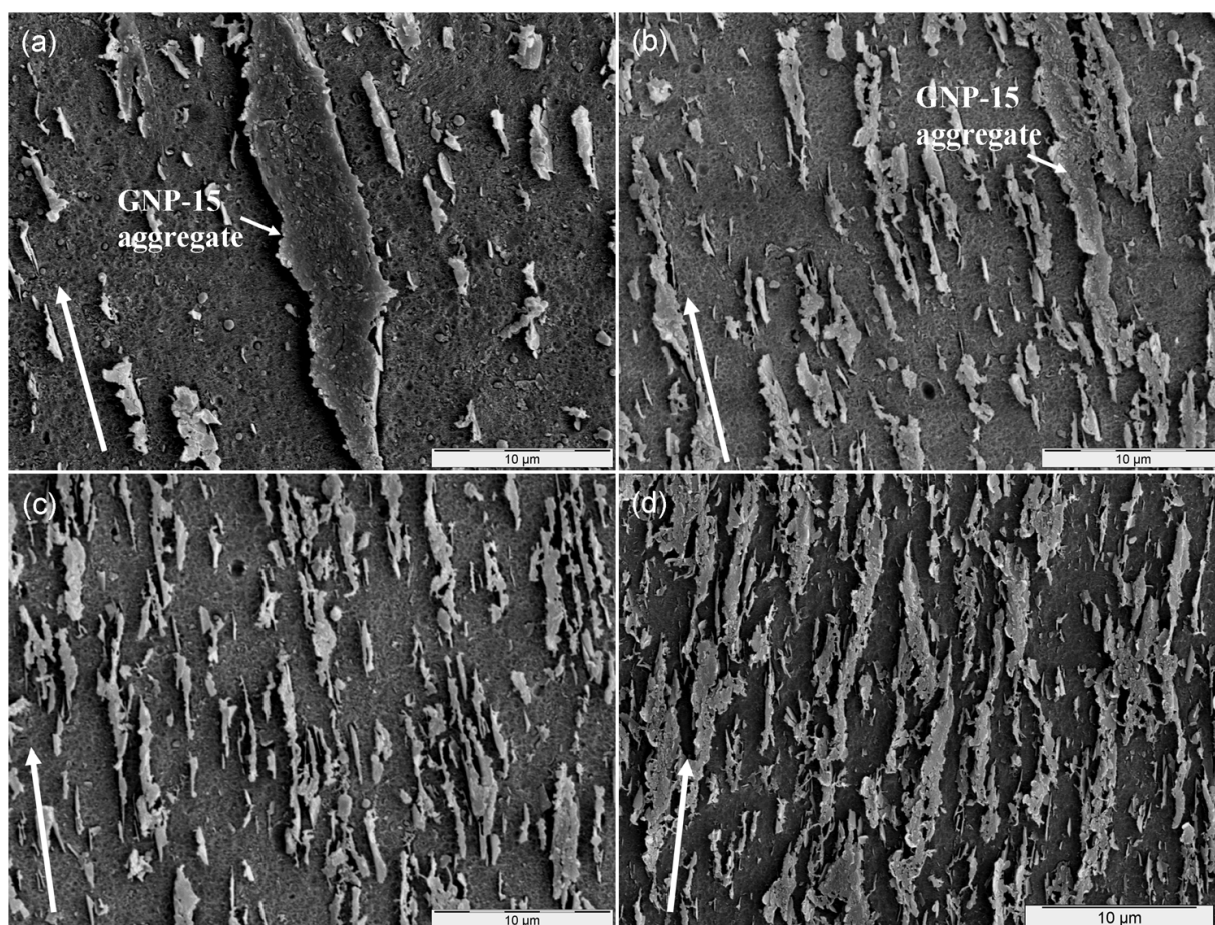


Fig. 15. Morphology of various HDPE/WaxGNP-15 nanocomposites at 5vol% GNP loading: (a) sonicated HDPE/GNP-15; (b) HDPE/WaxGNP-15 (10:90wt%); (c) HDPE/WaxGNP-15 (20:80wt%); (d) HDPE/WaxGNP-15 (30:70wt%). The arrow on the left bottom indicates the material flow direction during injection molding.

Fig. 15(b) to Fig. 15(d) compare the morphology of 5vol% HDPE/WaxGNP-15 nanocomposites with increasing wax content. It is clear to see that the number density of GNP-15 platelets is increasing as the wax content increases and big GNP-15 aggregates can no longer be detected. The disappearance of GNP aggregates as well as the increased GNP number density indicates that the re-aggregation of GNP-15 platelets is indeed prevented by the addition of the proper amount of wax coating on the surface. In this case, individual GNP-15 platelets can be dispersed uniformly in the polymer matrix. Meanwhile, the presence of well dispersed GNP-15 platelets significantly improves their interconnections in forming conductive pathways along the material flow direction, which is mainly responsible for the enhanced in-plane electrical conductivity of HDPE/WaxGNP-15 nanocomposites.

The morphology of the 5vol% HDPE/WaxGNP-15 (20:80wt%) nanocomposite in the center is presented in the Fig. 16. Compared with the morphology of the control sample (Fig. 12(d)), enhanced GNP-15 dispersion in HDPE is further confirmed, which results in disappearance of GNP-15 aggregates and higher GNP number density in HDPE. In this case, it is concluded that the wax coating method is capable of enhancing GNP dispersion in HDPE which leads to better mechanical and electrical properties in the resulting HDPE/GNP nanocomposites.

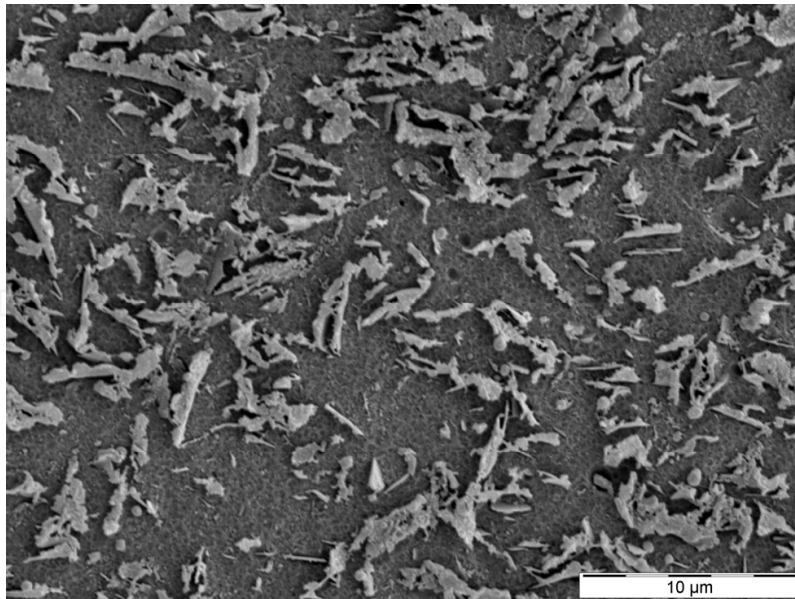


Fig. 16. Morphology of 5vol%HDPE/WaxGNP-15 (20:80wt%) sample in the center.

4. Conclusions

Various properties of HDPE/GNP nanocomposites made by melt-extrusion and injection molding were explored and analyzed in this book chapter, including mechanical properties, crystallization behaviors, thermal stability, thermal conductivity, and electrical conductivity. Results show some unique features of these injection molded nanocomposites. First of all, HDPE/GNP nanocomposites exhibit anisotropic thermal and electrical conductivity, that is, in-plane thermal and electrical conductivity were found to be much higher than the through-plane conductivity. Higher in-plane thermal and electrical properties of these nanocomposites are on the account of the alignment of GNP platelets along the material flow direction during injection molding, which were verified by their morphology. Secondly, it was found that the morphology of injection molded nanocomposites varies from the edge to the center. GNP platelets exhibit strong preferential alignment at the edge where the shear forces under injection molding are maximum while they are randomly orientated in the center where the shear forces are minimum. Additionally, sever GNP aggregation was detected in the melt-extrusion and injection molded samples, which is due to the insufficient shear force attainable during the processing conditions to shear GNP platelets apart and to achieve a uniform GNP dispersion. Regardless of this disadvantage, the technique of melt-extrusion and injection molding still remains as the major processing method used for manufacturing thermoplastics in industry because of its design flexibility, low cost and labor, short cycle time and minimum scrap loss. In order to improve the dispersion of GNP in HDPE, a wax coating technique was reported in this book chapter. It is concluded that the dispersion of GNP in HDPE was dramatically enhanced due to the steric repulsive forces between wax coated GNP platelets, which leads to the better electrical and mechanical properties in the resulting nanocomposites.

5. Acknowledgment

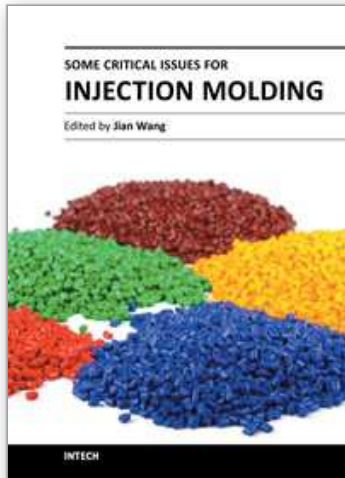
The authors gratefully acknowledgment the support of the Michigan Economic Development Commission, 21st Century Jobs Fund for partial support of this research. And the generous

help from Dr. Hiroyuki Fukushima, Dr. Wanjun Liu and Brian Rook in Composite Materials and Structures Center at Michigan State University is also gratefully appreciated.

6. References

- GNP is an exfoliated graphene nanoplatelet material obtained from XG Sciences, Inc., East Lansing, MI www.xgsciences.com, last access in 10/31/2011
- Balasubramanian, K., & Burghard, M. (2006). Biosensors based on carbon nanotubes *ANALYTICAL AND BIOANALYTICAL CHEMISTRY* 385, 3, pp. (452-468)
- Bang, J. H., & Suslick, K. S. (2010). Applications of Ultrasound to the Synthesis of Nanostructured Materials. *Advanced Materials*, 22, 10, pp. (1039-1059), 1521-4095
- Di Maio, E., Iannace, S., Sorrentino, L., & Nicolais, L. (2004). Isothermal crystallization in PCL/clay nanocomposites investigated with thermal and rheometric methods. *Polymer* 45, pp. (8893-8900), 0032-3861
- Fukushima, H. (2003). *Graphite nanoreinforcements in polymer nanocomposites*. PHD Thesis, Michigan State University, East Lansing, MI, USA
- Griffith, A. A. (1920). The phenomena of rapture and flaw in solids. *Phil. Trans. R. Soc. Lond. A*, 221, pp. (163-198)
- Hermant, M. C., Klumperman, B., Kyrylyuk, A. V., van der Schoot, P., & Koning, C. E. (2009). Lowering the percolation threshold of single-walled carbon nanotubes using polystyrene/poly(3,4-ethylenedioxythiophene): poly(styrene sulfonate) blends. *Soft Matter*, 5, pp. (878 - 885), 1744-683X
- Hussain, F., Hojjati, M., Okamoto, M., & Gorga, R. (2006). Review article: Polymer-matrix Nanocomposites, Processing, Manufacturing, and Application: An Overview. *Journal of Composite Materials*, 40, 17, pp. (1511-1575)
- I. Krupa, I. Novák, & Chodák, I. (2004). Electrically and thermally conductive polyethylene/graphite composites and their mechanical properties. *Synthetic Metals*, 145, pp. (245-252)
- Jiang, X., & Drzal, L. T. (2010). Multifunctional high density polyethylene nanocomposites produced by incorporation of exfoliated graphite nanoplatelets 1: Morphology and mechanical properties. *Polymer Composites*, 31, 6, pp. (1091-1098), 1548-0569
- Jiang, X., & Drzal, L. T. (2011). Improving Electrical Conductivity and Mechanical Properties of High Density Polyethylene through Incorporation of Paraffin Wax Coated Exfoliated Graphene Nanoplatelets and Multi-wall Carbon Nano-tubes. *Composites Part A: Applied Science and Manufacturing*, 42, 11, pp. (1840-1849), 1359-835X
- Jiang, X., & Drzal, L. T. (2011). Multifunctional high density polyethylene nanocomposites produced by incorporation of exfoliated graphite nanoplatelets 2: crystallization, thermal, and electrical properties. *submitted to the Journal of Polymer Composites*
- Jiang, X., & Drzal, L. T. (2011). Reduction in percolation threshold of injection molded High Density Polyethylene/Exfoliated Graphene Nanoplatelets composites by Solid State Ball Milling and Solid State Shear Pulverization. *Journal of Applied Polymer Science* In Press, Accepted Manuscript
- Kalaitzidou, K. (2006). *Exfoliated Graphene Nanoplatelets as Nanoreinforcement for Multifunctional Polypropylene Nanocomposites*. PHD Thesis, Michigan State University, East Lansing, MI, USA
- Kalaitzidou, K., Fukushima, H., & Drzal, L. T. (2007). Multifunctional polypropylene composites produced by incorporation of exfoliated graphite nanoplatelets. *Carbon*, 45, pp. (1446-1452)

- Kalaitzidou, K., Fukushima, H., & Drzal, L. T. (2007). A new compounding method for exfoliated graphite-polypropylene nanocomposites with enhanced flexural properties and lower percolation threshold. *Composites Science and Technology*, 67, pp. (2045-2051)
- Kashiwagi, T., Fagan, J., Douglas, J. F., Yamamoto, K., Heckert, A. N., Leigh, S. D., Obrzut, J., Du, F. M., Lin-Gibson, S., Mu, M. F., Winey, K. I., & Haggenueller, R. (2007). Relationship between dispersion metric and properties of PMMA/SWNT nanocomposites. *Polymer*, 48, 16, (Jul), pp. (4855-4866), 0032-3861
- Kim IH, Kim JH, & KB, K. (2005). Electrochemical characterization of electrochemically prepared ruthenium oxide/carbon nanotube electrode for supercapacitor application *Electrochemical and Solid State Letters*, 8, 7, pp. (A369-A372)
- Kim, J.-K., & Mai, Y.-W. (1991). High strength, high fracture toughness fibre composites with interface control – A review *Composites Science and Technology*, 41, 4, pp. (333-378)
- Kim, S., & Drzal, L. T. (2009). Comparison of Exfoliated Graphite Nanoplatelets (xGnP) and CNTs for Reinforcement of EVA Nanocomposites Fabricated by Solution Compounding Method and Three Screw rotating Systems *Journal of Adhesion Science and Technology*, 23, pp. (1623-1638)
- Mai, K., Li, J., & Zeng, H. (1994). Mechanical property and fracture morphology of fiber-reinforced polysulfone plasticized with acetylene-terminated sulfone. *Journal of Applied Polymer Science*, 52, 9, pp. (1279 - 1291)
- Peneva, Y., & Minkova, L. (2006). Non-isothermal and isothermal crystallization of nanocomposites based on functionalized polyethylenes. *Polymer Testing*, 25, 3, pp. (366-376), 0142-9418
- Piggott, M. R. (1980). *Load Bearing Fibre Composites*, Pergamon Press
- Singh, K. V., Pandey, R. R., Wang, X., Lake, R., Ozkan, C. S., Wang, K., & Ozkan, M. (2006). Covalent functionalization of single walled carbon nanotubes with peptide nucleic acid: Nanocomponents for molecular level electronics. *Carbon*, 44, 9, pp. (1730-1739), 0008-6223
- Vaia, R. A. (2003). Polymer nanocomposites open a new dimension for plastics and composites. *AMPTIAC Newsletter*, 6, 1, pp. (17-24)
- Wakabayashi, K., Pierre, C., & Dikin, D. A. (2008). Polymer-Graphite Nanocomposites: Effective Dispersion and Major Property Enhancement via Solid-State Shear Pulverization. *Macromolecules*, 41, pp. (1905-1908)
- Weibull, W. J. (1951). A statistical distribution function of wide applicability. *Journal of Applied Mechanics*, 18, (September), pp. (293-297)
- Xie, S. H., Liu, Y. Y., & Li, J. Y. (2008). Comparison of the effective conductivity between composites reinforced by graphene nanosheets and carbon nanotubes. *Applied Physics Letters*, 92, pp. (243121-3), 1077-3118
- Yang, S., Taha-Tijerina, J., Serrato-Diaz, V., Hernandez, K., & Lozano, K. (2007). Dynamic mechanical and thermal analysis of aligned vapor grown carbon nanofiber reinforced polyethylene. *Composites Part B: Engineering*, 38, pp. (228-235), 1359-8368
- Yao, X., Wu, H., Wang, J., Qu, S., & Chen, G. (2006). Carbon nanotube/poly(methyl methacrylate) (CNT/PMMA) composite electrode fabricated by in situ polymerization for microchip capillary electrophoresis *Chemistry - A European Journal*, 13, 3, pp. (846 - 853)



Some Critical Issues for Injection Molding

Edited by Dr. Jian Wang

ISBN 978-953-51-0297-7

Hard cover, 270 pages

Publisher InTech

Published online 23, March, 2012

Published in print edition March, 2012

This book is composed of different chapters which are related to the subject of injection molding and written by leading international academic experts in the field. It contains introduction on polymer PVT measurements and two main application areas of polymer PVT data in injection molding, optimization for injection molding process, Powder Injection Molding which comprises Ceramic Injection Molding and Metal Injection Molding, and some special techniques or applications in injection molding. It provides some clear presentation of injection molding process and equipment to direct people in plastics manufacturing to solve problems and avoid costly errors. With useful, fundamental information for knowing and optimizing the injection molding operation, the readers could gain some working knowledge of the injection molding.

How to reference

In order to correctly reference this scholarly work, feel free to copy and paste the following:

Xian Jiang and Lawrence T. Drzal (2012). Properties of Injection Molded High Density Polyethylene Nanocomposites Filled with Exfoliated Graphene Nanoplatelets, Some Critical Issues for Injection Molding, Dr. Jian Wang (Ed.), ISBN: 978-953-51-0297-7, InTech, Available from: <http://www.intechopen.com/books/some-critical-issues-for-injection-molding/properties-of-injection-molded-high-density-polyethylene-nanocomposites-filled-with-exfoliated-graph>

INTECH
open science | open minds

InTech Europe

University Campus STeP Ri
Slavka Krautzeka 83/A
51000 Rijeka, Croatia
Phone: +385 (51) 770 447
Fax: +385 (51) 686 166
www.intechopen.com

InTech China

Unit 405, Office Block, Hotel Equatorial Shanghai
No.65, Yan An Road (West), Shanghai, 200040, China
中国上海市延安西路65号上海国际贵都大饭店办公楼405单元
Phone: +86-21-62489820
Fax: +86-21-62489821

© 2012 The Author(s). Licensee IntechOpen. This is an open access article distributed under the terms of the [Creative Commons Attribution 3.0 License](#), which permits unrestricted use, distribution, and reproduction in any medium, provided the original work is properly cited.

IntechOpen

IntechOpen